

Design of Yagi-Uda Antenna with Multiple Driven Elements

Huadong Guo and Wen Geyi*

Abstract—In this paper, we present a novel design for an end-fire antenna, which generalizes the concept of conventional Yagi-Uda antenna by introducing multiple driven elements. Through using the method of maximum power transmission efficiency, the optimal distribution of excitations for the multiple driven elements can be obtained, and the end-fire gain of the array can be significantly improved in comparison with the conventional Yagi-Uda antenna with a single driven element. In order to demonstrate the new idea, two different types of antenna arrays are designed and fabricated. The first design uses a split-ring resonator (SRR) as radiating element. Compared to similar planar Yagi-Uda SRR antenna arrays previously reported, the number of antenna elements can be reduced from fifteen to eight, and the longitudinal dimension is significantly reduced by 46% while the same performances are maintained with the gain reaching 11.7 dBi at 5.5 GHz. In the second design, printed half-wavelength dipoles are used as the antenna elements. It is shown that an eight-element dipole array with four driven elements has a peak gain of 13.4 dBi at 2.45 GHz, which is 1.8 dB higher than the conventional printed Yagi-Uda dipole antenna array with the same number of elements.

1. INTRODUCTION

Yagi-Uda antenna is known for its high gain, low cost, and end-fire radiation, which usually consists of one driven element, one reflector, and several directors [1–3]. In order to maximize the gain and front-to-back ratio (FBR) of Yagi-Uda antenna, the size and geometry of elements, and the spacing among elements must be optimized [4, 5]. Although the dipole has been commonly used as radiating elements of Yagi-Uda antenna, there are many other options for selecting the radiating elements. For example, a rectangular microstrip patch can be used as the radiating element of Yagi-Uda antenna [6]. The design has many advantages such as low profile, light weight, and low cost. One apparent drawback of the design is that it cannot really achieve the end-fire radiation due to the existence of a ground plane. Many other low profile Yagi-Uda antennas have also been investigated [7–25]. Among them, a planar Yagi-Uda antenna was proposed by using a split-ring resonator (SRR) as the radiating element [25]. It consists of 15 elements and has an end-fire gain of 11.3 dBi at 5.5 GHz, and the width is only a quarter wavelength at its center frequency. Although the transverse dimension is considerably reduced in the design, the number of directors must be big enough to ensure that the performances are comparable to those of a Yagi-Uda antenna consisting of half-wavelength dipoles. Recently, a printed dipole array operating at 2.45 GHz was introduced in [26], in which the end-fire gain and FBR can be optimized by using the method of maximum power transmission efficiency (MMPTE) [27, 28].

In this paper, we propose a novel design for end-fire antennas which are similar to conventional Yagi-Uda antennas but have more than one driven elements. We call the design generalized Yagi-Uda antenna. To demonstrate the advantages of the generalized Yagi-Uda antenna, two designs are presented. The first design is based on SRR elements, working at 5.5 GHz for wireless local area network (WLAN) and includes five driven elements. Through the control of amplitude and phase distribution of driven

Received 30 January 2019, Accepted 19 April 2019, Scheduled 25 April 2019

* Corresponding author: Geyi Wen (wgy@nuist.edu.cn).

The authors are with the Nanjing University of Information Science and Technology, Nanjing 210044, China.

elements, the size of the classical Yagi-Uda array can be significantly reduced. Compared with a similar design in [25], the longitudinal dimension of arrays is reduced by 46% while maintaining the same lateral dimension and end-fire gain. It is also demonstrated that the end-fire gain and FBR can be further improved by increasing the number of directors when the number of driven elements is kept the same. The second design operates at 2.45 GHz for Wi-Fi applications and makes use of printed half-wavelength dipole as radiating element. It has four driven elements, one reflector, and three directors. The measurements and simulations indicate that the end-fire gain reaches 13.4 dBi, which is 1.8 dB higher than the traditional printed dipole Yagi-Uda antenna with the same number of elements and size.

2. DESIGN METHOD

A key step in the design of a generalized Yagi-Uda antenna is to determine the excitations for the multiple driven elements. To obtain an optimized distribution of excitations for the multiple driven elements, MMPTE can be used. MMPTE is based on the fact that all wireless systems are designed to maximize the power transmission efficiency between the transmitter and receiver, and the power transmission efficiency can thus be considered as a natural performance index for antenna design. MMPTE has been widely used in the design of near-field focused antennas [29], wireless power transmission systems in complicated environments [30], smart antennas [31], and beam-shaping antennas in the far- and near-field regions [32].

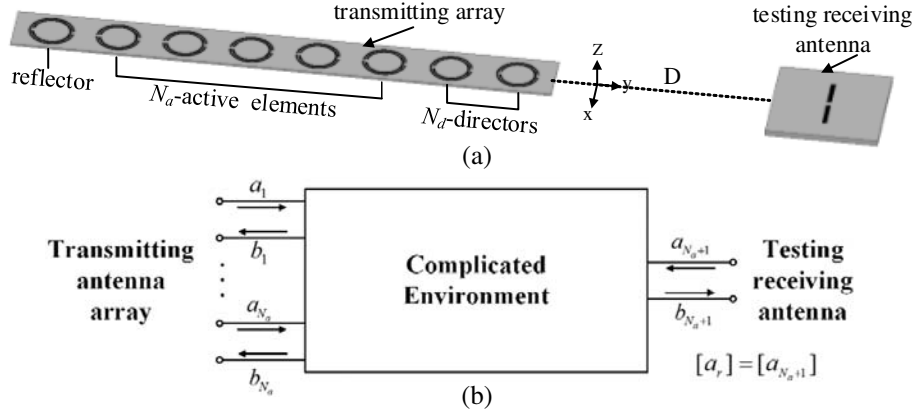


Figure 1. Power transmission between transmitting antenna array and receiving antenna. (a) Setup. (b) Equivalent network.

For clarity and completeness, we give a brief introduction to the MMPTE. Consider the wireless power transmission system shown in Fig. 1, where the antenna array to be designed is used for transmitting, and a test antenna, separated by a distance D from the transmitting antenna, is utilized for receiving. The test receiving antenna is located in the far-field region of transmitting array and positioned in the direction where the gain needs to be boosted. The whole system constitutes a network containing $N_a + 1$ ports, where N_a denotes the number of driven elements and can be characterized by scattering parameters as follows

$$\begin{bmatrix} [b_t] \\ [b_r] \end{bmatrix} = \begin{bmatrix} [S_{tt}] & [S_{tr}] \\ [S_{rt}] & [S_{rr}] \end{bmatrix} \begin{bmatrix} [a_t] \\ [a_r] \end{bmatrix}, \quad (1)$$

where

$$\begin{aligned} [a_t] &= [a_1, a_2, \dots, a_{N_a}]^T, \\ [a_r] &= [a_{N_a+1}], \end{aligned}$$

and

$$\begin{aligned} [b_t] &= [b_1, b_2, \dots, b_{N_a}]^T, \\ [b_r] &= [b_{N_a+1}], \end{aligned}$$

are respectively the normalized incident and reflected waves for the wireless power transmission system. Subscript ‘ t ’ and ‘ r ’ represent the transmitting and receiving antennas, respectively, and superscript ‘ T ’ stands for the transpose operation. The power transmission efficiency (PTE), denoted by η , between the transmitting antenna array and receiving antenna is defined as the ratio of the power delivered to the load of the receiving antenna to the total input power of the transmitting antenna array

$$\eta = \frac{\frac{1}{2}(|[b_r]|^2 - |[a_r]|^2)}{\frac{1}{2}(|[a_t]|^2 - |[b_t]|^2)}. \quad (2)$$

Assume that the receiving antenna is well matched, so we have $[a_r] = 0$. Making use of Eq. (1), Eq. (2) can be written as the Rayleigh quotient as follows

$$\eta = \frac{([A][a_t], [a_t])}{([B][a_t], [a_t])}, \quad (3)$$

where (\cdot, \cdot) denotes the usual inner product of two column vectors; $[A]$ and $[B]$ are two matrices defined by

$$[A] = [S_{rt}]^H [S_{rt}], \quad [B] = I - [S_{tt}]^H [S_{tt}],$$

where superscript ‘ H ’ denotes the Hermitian operation, and I is the identity matrix. If the transmitting array is well matched at all ports, then we have $[S_{tt}] = [0]$, $[B] = I$. If the PTE reaches an extremum, Eq. (3) is reduced to an eigenvalue equation

$$[A][a_t] = \eta [a_t] \quad (4)$$

from variational analysis. Here matrix $[A]$ can be obtained by simulation tools or by measurements if the system is too complicated to be handled by a computer [30]. By solving the eigenvalue of Equation (4), the maximum possible PTE can be determined. Note that the mutual couplings among the transmitting antenna elements and environmental factors have already been included in the scattering matrix. Also note that Equation (4) has only one positive eigenvalue, and the rest are zeros since the rank of matrix $[A]$ is unit in this case. Therefore, the unique nonzero eigenvalue of Equation (4) gives the maximum power transmission efficiency between the antenna array and the test receiving antenna, and the corresponding eigenvector is the optimal excitation for the antenna array in the sense that the PTE between the transmitting array and test receiving antenna is maximized. By designing a feeding network that realizes the optimized distribution of excitations for the driven elements, the maximum gain can be achieved in the direction where the test receiving antenna is positioned for a fixed arrangement of the antenna elements. The details of the optimization theory are given in [27] and [28].

3. ANTENNA DESIGNS AND RESULTS

3.1. Generalized Yagi-Uda SRR Antenna

A Yagi-Uda antenna using split-ring resonators (SRRs) has been studied in [25]. The lateral dimension of SRR is only a quarter wavelength at its second resonance frequency, while its radiation characteristics are similar to a half-wavelength dipole [33]. We now show that the longitudinal dimension of SRR Yagi-Uda antenna can be further reduced by introducing multiple driven elements. The first design is named array 1, and the SRR element used is shown in Fig. 2, where the average radius r is calculated by $r = \lambda_0/11$ (λ_0 is the working wavelength in free space) so that its radiation resistance is close to 50Ω [25]. Thus the radius is determined to be 5.2 mm when the working frequency is 5.5 GHz. The dimensions of the SRR are as follows: the strip width $w = 0.5$ mm; the internal and external ring spacing $d = 0.35$ mm; the split width of external ring $c = 1.3$ mm; and the width of the port $g = 0.762$ mm.

Array 1 consists of five driven elements, one reflector, and two directors. For a fair comparison, the sizes of directors and reflector are selected to be the same as in [25]. The spacing between driven elements is selected to be 17.8 mm; the size of reflector is selected to be 3% larger than driven elements; the spacing between the reflector and driven element next to it is set to 18 mm; the size of directors is 4% smaller than the driven elements; and the spacing between two adjacent directors is chosen to

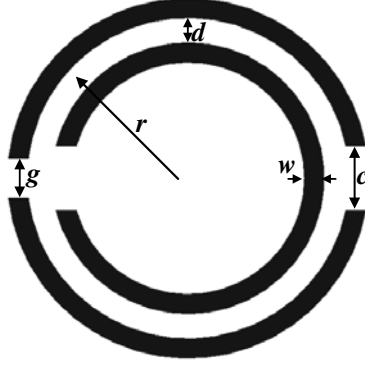


Figure 2. SRR for the driven element.

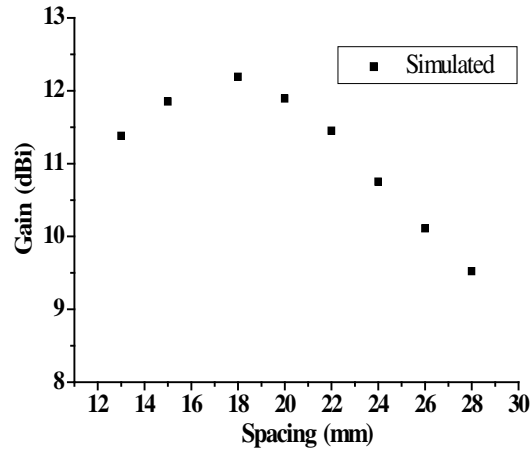


Figure 3. The relationship between the spacing between driven elements and the end-fire gain.

be 17.5 mm. Note that the sizes of antenna elements and spacings among the parasitic elements are determined by empirical formula [4, 5]. The optimized spacing between adjacent driven elements can be obtained by simulations using the HFSS. It is easy to see from Fig. 3 that the maximum end-fire gain is reached when the inter-element spacing is about 18 mm, explaining why this number is chosen in our design. The optimized parameters of the different type of elements are listed in Table 1.

Table 1. Parameters of the SRRs.

Parameter	reflector	driven	director
w (mm)	0.52	0.5	0.48
d (mm)	0.31	0.3	0.29
r (mm)	5.36	5.2	5

To determine the excitations for the driven elements, a six-port power transmission system can be formed by using the five driven elements ($N_a = 5$) for transmitting and a test antenna for receiving. By solving the eigenvalue of Equation (4), the optimized excitations can be obtained. The optimized results of the distribution of excitations for the proposed antenna array are listed in Table 2 in which the realized distribution of excitations of the feeding network is also shown and agrees with the optimized one. Because the maximum radiation direction is in the positive y -axis with the same spacing between the driven elements, the amplitude of the excitations gradually increases while the phase difference between driven elements is approximately the same.

Table 2. Distribution of excitations.

Port No.	Optimized excitations	Realized excitation of feeding network
1	0.4∠160	0.39∠160.7
2	0.43∠17.6	0.42∠17.2
3	0.39∠ - 110.1	0.39∠ - 110.8
4	0.43∠134.6	0.43∠133.7
5	0.56∠0	0.56∠0

Figures 4(a) and 4(b) show the side and top views of the optimized antenna array 1. For comparison with [25], the radiating elements are etched on an ArlonCU 250LX dielectric substrate with thickness of $h_1 = 0.49$ mm, relative permittivity of $\epsilon_r = 2.43$, and loss tangent of 0.0022. The length of substrate 1 is $L_s = 140$ mm ($2.54\lambda_0$), and the width is $W_s = 14$ mm ($0.25\lambda_0$). Rogers-4003 dielectric substrate 2 is used for the feeding network, with thickness of $h_2 = 0.762$ mm, relative permittivity of $\epsilon_r = 3.55$, and loss tangent of 0.0027. The length of substrate 2 is $L_f = 90$ mm, and the width $W_f = 12$ mm. The microstrip feeding network is deployed on substrate 2 with a metal ground to realize the optimized distribution of excitation. For the current design, substrate 2 is glued to substrate 1. In practice, 3D printing technique can be used to build the system as a whole. Note that the feeding network can also be realized by other feeding methods. For example, one can use a separate feeding circuit consisting of phase shifters and attenuators as illustrated in [31].

A photograph of the fabricated array 1 is shown in Fig. 5. The simulated and measured reflection coefficients are shown in Fig. 6. It can be seen that the reflection coefficient S_{11} is less than -10 dB

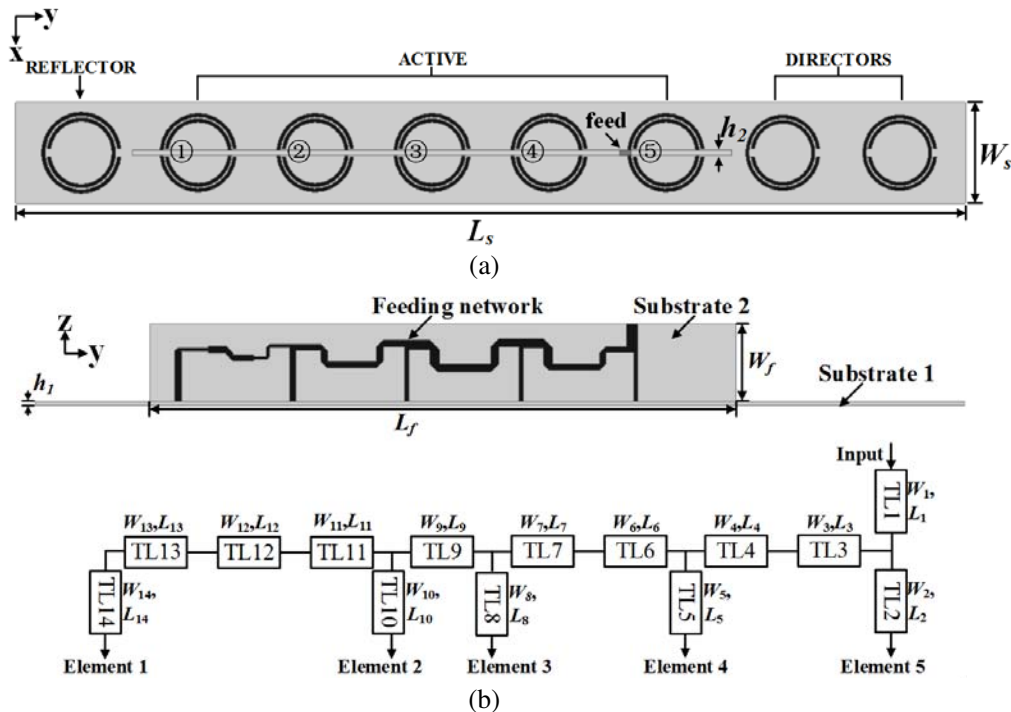


Figure 4. Array 1: Geometry of the generalized Yagi-Uda SRR antenna. ($N_a = 5$, $N_d = 2$). (a) Top view. (b) Side view and schematic of feeding network. The parameters are (mm): $W_1 = 1.78$, $L_1 = 3.5$; $W_2 = 0.9$, $L_2 = 8.5$; $W_3 = 0.9$, $L_3 = 15.8$; $W_4 = 1.4$, $L_4 = 8.1$; $W_5 = 0.66$, $L_5 = 8.3$; $W_6 = 1.2$, $L_6 = 16.7$; $W_7 = 1.5$, $L_7 = 8.3$; $W_8 = 0.66$, $L_8 = 8.3$; $W_9 = 1$, $L_9 = 23$; $W_{10} = 0.95$, $L_{10} = 8.45$; $W_{11} = 0.45$, $L_{11} = 8$; $W_{12} = 1$, $L_{12} = 8.35$; $W_{13} = 0.5$, $L_{13} = 4.7$; $W_{14} = 1$, $L_{14} = 8.35$.



Figure 5. Array 1: Generalized Yagi-Uda SRR antenna ($N_a = 5$, $N_d = 2$).

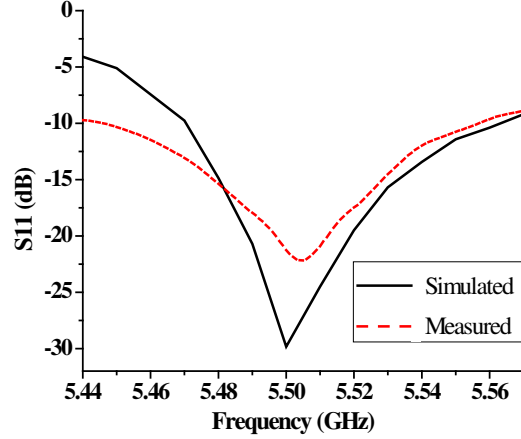


Figure 6. Simulated and measured reflection coefficients of the antenna array 1.

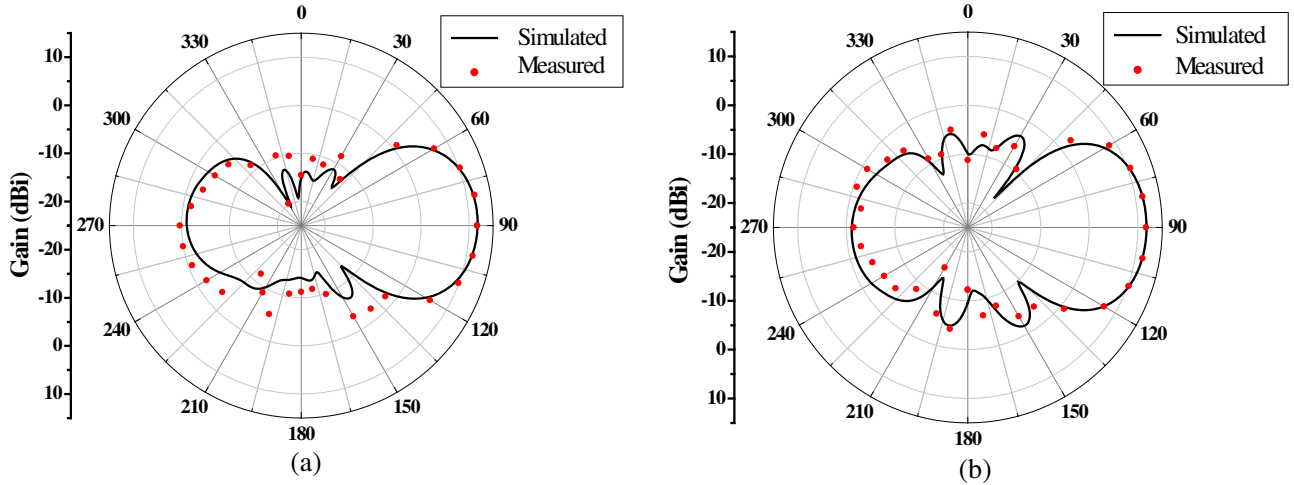


Figure 7. Radiation patterns of antenna array 1 at 5.5 GHz on (a) E -plane (xy) and (b) H -plane (yz).

from 5.44 to 5.56 GHz (bandwidth 2.4%). The measured radiation patterns on the E -plane and H -plane are shown in Fig. 7(a) and (b), respectively, which agree well with the simulated ones. Moreover, the antenna exhibits an end-fire gain of 11.7 dBi with a radiation efficiency of 94% and FBR of 13.4 dB (see Fig. 7). Compared with [25], the longitudinal dimension of proposed antenna array is reduced by 46% while the same end-fire gain and lateral dimension are maintained. Fig. 8 indicates that the measured end-fire gain varies from 8.7 to 12 dBi within the working band.

As the number of directors increases, the end-fire gain increases accordingly. Fig. 9 shows how the gain changes with the number of directors. The end-fire gain increases from 11.7 to 13.3 dBi as the number of directors increases from 2 to 9. For $N_a = 5$ and $N_d = 9$, the end-fire gain is 2 dB higher than the fifteen-element array in [25]. To further improve the FBR and end-fire gain, a generalized

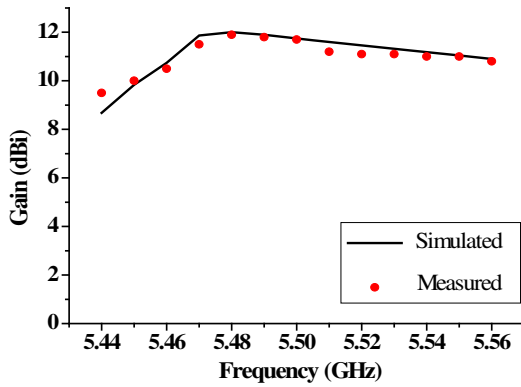


Figure 8. End-fire gains for the designed array 1.

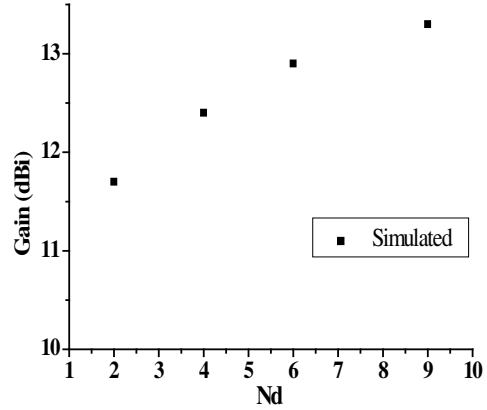


Figure 9. End-fire gains of the generalized Yagi-Uda SRR arrays ($N_a = 5$).

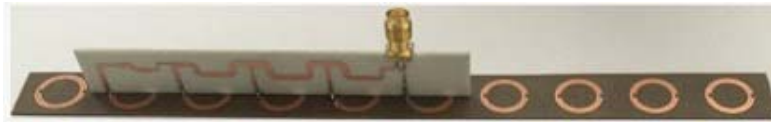


Figure 10. Array 2: ten-element generalized Yagi-Uda SRR array ($N_a = 5, N_d = 4$).

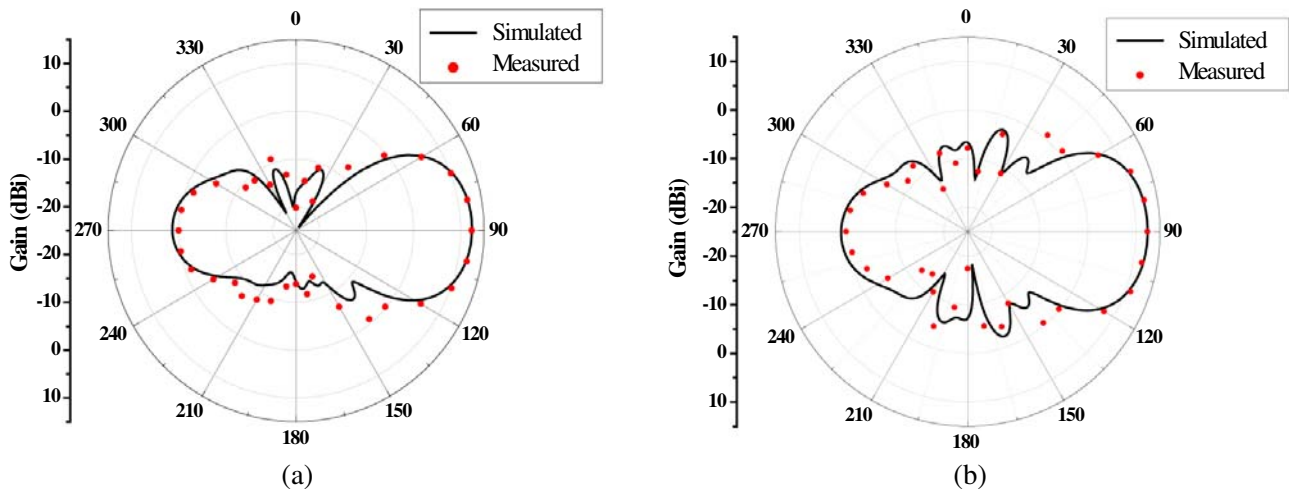


Figure 11. Radiation patterns of antenna array 2 at 5.5 GHz on (a) E -plane (xy) and (b) H -plane (yz).

Yagi-Uda SRR antenna with five driven elements and four directors, named array 2, has been designed and is shown in Fig. 10. The longitudinal dimension is increased to 175 mm ($3.18\lambda_0$), but it is still 31% less than in [25]. The measured and simulated E -plane and H -plane radiation patterns are shown in Figs. 11(a) and (b). The measured end-fire gain is increased to 12.4 dBi, which is 1.1 dB higher than in [25], and the FBR is 14.8 dB. It should be mentioned that increasing the number of reflectors does not have substantial improvements on the antenna performances.

The comparison between the generalized Yagi-Uda arrays and conventional planar Yagi-Uda arrays is also shown in Table 3. Compared with the antenna array in [14], the gain of array 1 is 1.3 dB higher, while its dimensions are considerably reduced.

Table 3. Performance comparison of antennas.

	Array 1	Array 2	[25]	[14]
No. of elements	8	10	15	12
Frequency (GHz)	5.5	5.5	5.5	5.5
Bandwidth	2.4	2.4	2.7	11.7
Efficiency (%)	94	94	84	-
Gain (dBi)	11.7	12.4	11.3	10.4
FBR (dB)	13.4	14.8	14	10
Length	$2.54\lambda_0$	$3.18\lambda_0$	$4.6\lambda_0$	$3.47\lambda_0$
Width	$0.25\lambda_0$	$0.25\lambda_0$	$0.25\lambda_0$	$1.73\lambda_0$

3.2. Generalized Yagi-Uda Dipole Antenna

Our second design uses half-wavelength dipoles as the antenna elements. An eight-element generalized Yagi-Uda antenna with four driven elements and three directors ($N_a = 4$, $N_d = 3$), operating at 2.45 GHz for Wi-Fi applications, is investigated. The four driven elements ($N_a = 4$) plus the test receiving antenna constitute a five-port power transmission system, which is used to determine the optimized distribution of excitations. The radiating elements are printed on Rogers-4003 substrate 1, with relative permittivity of $\epsilon_r = 3.55$ and loss tangent of 0.0027. Similarly, a microstrip feeding network is designed on Rogers-4003 substrate 2 with a metal ground to realize the optimized distribution of excitation. The configuration of the generalized Yagi-Uda dipole antenna array and a photo of the fabricated antenna are illustrated in Fig. 12. The optimized parameters of the design are listed in Table 4. The realized distribution of excitations of the feeding network is shown in Table 5, which agrees well with the optimized one.

Table 4. Geometrical parameters of the designed array.

L_s	W_s	W_d	L_r	L_a	W_f
308 mm	60 mm	1.4 mm	49 mm	44.6 mm	12 mm
L_d	S_r	S_a	S_d	L_f	h_1, h_2
40 mm	44.2 mm	45.8 mm	39.2 mm	168 mm	1.524 mm

Table 5. Distribution of excitations.

Port No.	Optimized excitations	Realized excitations of feeding network
1	$0.32\angle 73.3$	$0.32\angle 72.5$
2	$0.41\angle -89.7$	$0.41\angle -90.1$
3	$0.49\angle 131.4$	$0.49\angle 130.8$
4	$0.7\angle 0$	$0.69\angle 0$

Figure 13 shows that the measured reflection coefficient of the generalized Yagi-Uda dipole array is below -10 dB from 2.35 to 2.51 GHz (bandwidth 6.6%). The measured and simulated results for radiation patterns on the E -plane and H -plane are plotted in Figs. 14(a) and (b), respectively. The measured end-fire gain and FBR reach 13.4 dBi and 16.4 dB, respectively (with radiation efficiency of 96.5%), which agree well with the simulated results. A comparison with conventional Yagi-Uda dipole array with the same number of elements is also made in Fig. 14, which indicates that the end-fire gain

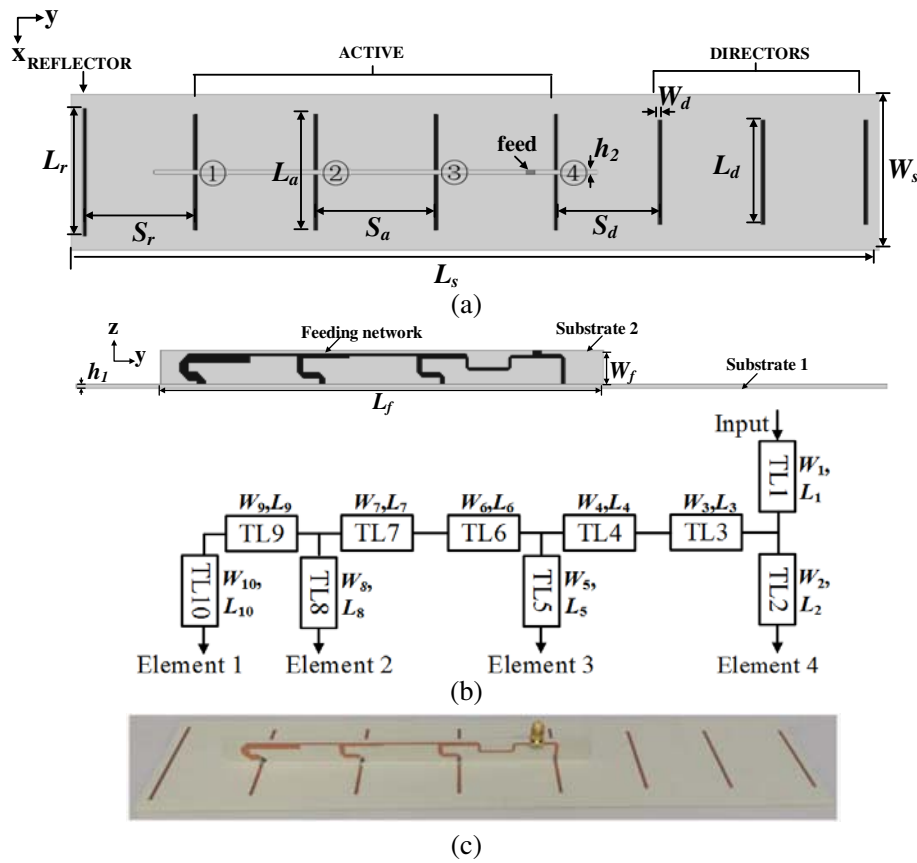


Figure 12. The configuration of generalize Yagi-Uda dipole antenna array operating at 2.45 GHz. (a) Top view. (b) Side view and schematic of feeding network. The parameters are (mm): $W_1 = 3.37$, $L_1 = 1.65$; $W_2 = 1.4$, $L_2 = 18.1$; $W_3 = 1.05$, $L_3 = 33.1$; $W_4 = 2$, $L_4 = 18.4$; $W_5 = 1.85$, $L_5 = 18.7$; $W_6 = 1$, $L_6 = 25.7$; $W_7 = 1.8$, $L_7 = 18.7$; $W_8 = 2.2$, $L_8 = 18.4$; $W_9 = 1$, $L_9 = 19$; $W_{10} = 3.37$, $L_{10} = 41$. (c) Photo.

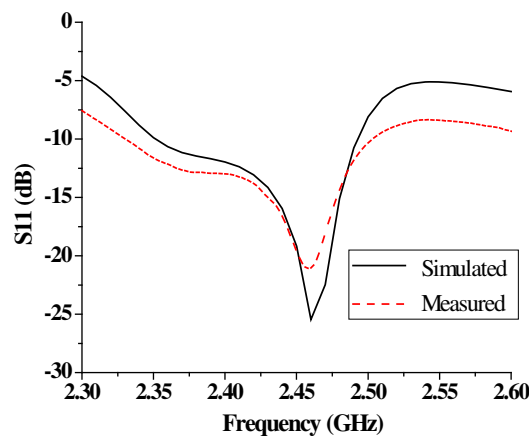


Figure 13. Simulated and measured reflection coefficients of the antenna array.

and FBR of the generalized design are respectively 1.8 and 6.8 dB higher than the conventional Yagi-Uda dipole array ($N_a = 1$, $N_d = 6$). Fig. 15 indicates that the measured and simulated end-fire gains change from 11.7 to 13.5 dBi in the operating frequency band.

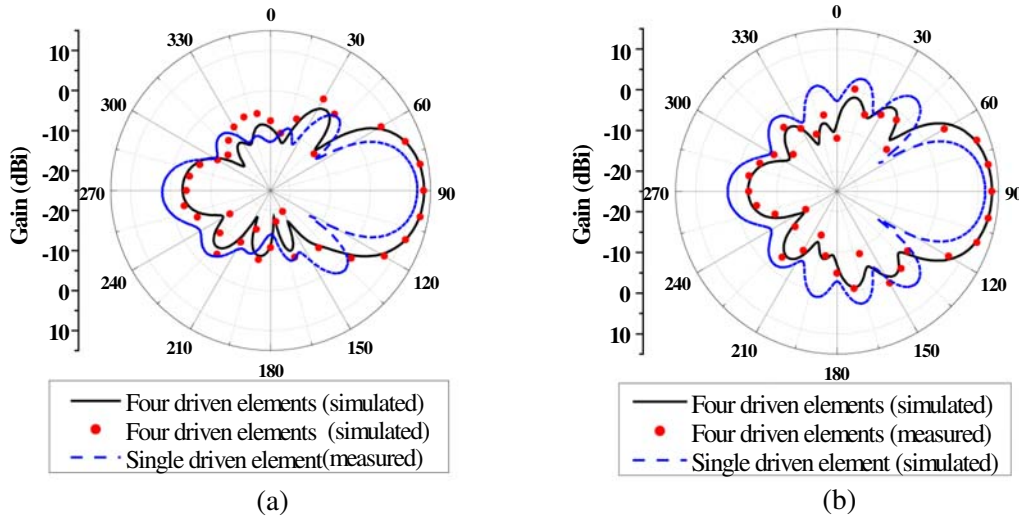


Figure 14. Radiation patterns of proposed antenna array at 2.45 GHz on (a) E -plane (xy) and (b) H -plane (yz).

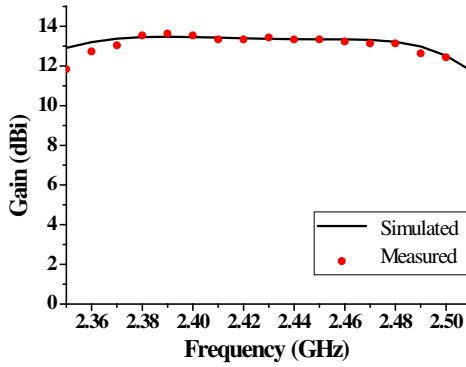


Figure 15. End-fire gains for the generalized Yagi-Uda dipole array ($N_a = 4$, $N_d = 3$).

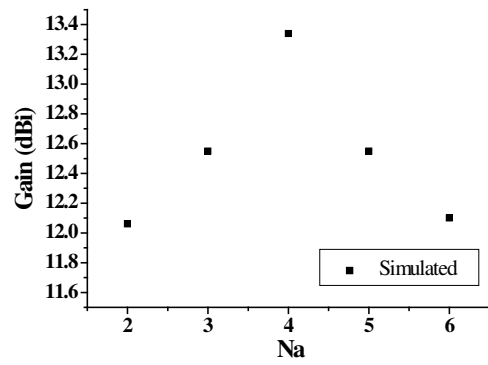


Figure 16. End-fire gains of the generalized Yagi-Uda dipole array ($N_a = 2, 3, 4, 5, 6$; $N_d = 5, 4, 3, 2, 1$, correspondingly).

It would be interesting to investigate the relationship between the number of driven elements and the end-fire gain when the total number of radiating elements is fixed. Fig. 16 shows how the end-fire gain changes with the number of driven elements. As the number of driven elements N_a increases from 2 to 4 (the number of directors N_d correspondingly decreases from 5 to 3), the end-fire gain increases from 12 to 13.4 dBi at 2.45 GHz. The end-fire gain starts to decrease if the number of driven elements further increases. This explains why four driven elements are selected in the design of the eight-element dipole array.

4. CONCLUSION

In this paper, the design concept of the conventional Yagi-Uda antenna is generalized by introducing multiple driven elements. The distribution of excitations for the generalized Yagi-Uda antenna is optimized by using MMPTE. In order to demonstrate the advantages of the new idea, two different types of antenna arrays are designed and fabricated. The first design uses SRR as radiating elements, which has five driven elements, one reflector, and two directors, working at 5.5 GHz for WLAN applications. Compared to similar planar Yagi-Uda antenna arrays previously reported, the number of antenna elements can be reduced from fifteen to eight, and the longitudinal dimension is significantly reduced

by 46%. It is also shown that the end-fire gain and FBR can be further improved by increasing the number of directors. The second design uses printed dipole as antenna elements, which includes four driven elements, one reflector, and three directors and operates at 2.45 GHz for Wi-Fi applications. The end-fire gain and FBR are respectively 1.8 dB and 6.8 dB higher than the conventional Yagi-Uda dipole antenna with the same number of radiating elements.

REFERENCES

1. Uda, S., "On the wireless beam of short electric waves," *J. Inst. Elec. Eng.*, Vol. 452, 273–282, Mar. 1926.
2. Uda, S., "On the wireless beam of short electric waves," *J. Inst. Elect. Eng.*, Vol. 472, 1209–1219, Nov. 1927.
3. Yagi, H., "Beam transmission of the ultra short waves," *Proc. IRE*, Vol. 16, No. 6, 715–741, Jun. 1928.
4. Cheng, D. K. and C. A. Chen, "Optimum element spacings for Yagi-Uda arrays," *IEEE Trans. Antennas Propag.*, Vol. 21, No. 5, 615–623, Sep. 1973.
5. Chen, C. A. and D. K. Cheng, "Optimum element lengths for Yagi-Uda arrays," *IEEE Trans. Antennas Propag.*, Vol. 23, No. 1, 8–15, Jan. 1975.
6. Huang, J., "Planar microstrip Yagi array antenna," *Proc. IEEE Antennas Propag. Soc. Int. Symp.*, Vol. 2, 894–897, Jun. 1989.
7. Densmore, A. and J. Huang, "Microstrip Yagi antenna for mobile satellite service," *IEEE Antennas and Propagation Society Int. Symp.*, Vol. 2, 616–619, Jun. 1991.
8. Huang, J. and A. Densmore, "Microstrip Yagi antenna for mobile satellite vehicle application," *IEEE Trans. Antennas Propag.*, Vol. 39, No. 7, 1024–1030, Jul. 1991.
9. Ke, S. and K. Wong, "Rigorous analysis of rectangular microstrip antennas with parasitic patches," *IEEE Antennas Propag. Society Int. Symp.*, Vol. 2, 968–971, Jun. 1995.
10. Gray, D., J. Lu, and D. Thiel, "Electronically steerable Yagi-Uda microstrip patch antenna array," *IEEE Trans. Antennas Propag.*, Vol. 46, No. 5, 605–608, May 1998.
11. Deal, W. R., N. Kaneda, J. Sor, Y. Qian, and T. Itoh, "A new quasi-Yagi antenna for planar active antenna arrays," *IEEE Trans. Microw. Theory Techn.*, Vol. 48, No. 6, 910–918, Jun. 2000.
12. Grajek, P. R., B. Schoenlinner, and G. M. Rebeiz, "A 24 GHz high-gain Yagi-Uda antenna array," *IEEE Trans. Antennas Propag.*, Vol. 52, No. 5, 1257–1261, May 2004.
13. De Jean, G. and M. Tentzeris, "A new high-gain microstrip Yagi array antenna with a high front-to-back (F/B) ratio for WLAN and millimeter wave applications," *IEEE Trans. Antennas Propag.*, Vol. 55, No. 2, 298–304, Feb. 2007.
14. Liu, J. H. and Q. Xue, "Microstrip magnetic dipole Yagi array antenna with endfire radiation and vertical polarization," *IEEE Trans. Antennas Propag.*, Vol. 61, No. 3, 1140–1147, Mar. 2013.
15. Ding, Y., Y. C. Jiao, B. Li, and L. Zhang, "Folded triple-frequency quasi-Yagi-type antenna with modified CPW-to-CPS transition," *Progress In Electromagnetics Research Letters*, Vol. 37, 143–152, 2013.
16. Wang, Z. D., X. L. Liu, Y. Z. Yin, J. H. Wang, and Z. Li, "A novel design of folded dipole for broadband printed Yagi-Uda antenna," *Progress In Electromagnetics Research C*, Vol. 46, 23–30, 2014.
17. Wang, H., S. F. Liu, W. T. Li, and X. W. Shi, "Design of a wideband planar microstrip-fed quasi-Yagi antenna," *Progress In Electromagnetics Research Letters*, Vol. 46, 19–24, 2014.
18. Zhang, S., Z. Tang, and Y. Yin, "Wideband planar printed quasi-Yagi antenna with band-notched characteristic," *Progress In Electromagnetics Research Letters*, Vol. 48, 137–143, 2014.
19. Hu, Z. X., Z. X. Shen, W. Wu, and J. Lu, "Low-profile top-hat monopole Yagi antenna for end-fire radiation," *IEEE Trans. Antennas Propag.*, Vol. 63, No. 7, 2851–2857, Jul. 2015.

20. Hu, Z. X., W. W. Wang, Z. X. Shen, and W. Wu, "Low-profile helical quasi-Yagi antenna array with multibeams at the endfire direction," *IEEE Antennas Wireless Propag. Lett.*, Vol. 16, 1241–1244, May 2017.
21. Yeo, J. and J. I. Lee, "Bandwidth enhancement of double-dipole quasi-yagi antenna using stepped slotline structure," *IEEE Antennas Wireless Propag. Lett.*, Vol. 15, 694–697, Mar. 2016.
22. Wu, Y., M. Qu, L. Jiao, Y. Liu, and Z. Ghassemlooy, "Graphene-based Yagi-Uda antenna with reconfigurable radiation patterns," *AIP Advances*, Vol. 6, 065308:1–11, 2016.
23. Zhao, T. H., Y. Xiong, X. Yu, and H. H. Chen, "A broadband planar quasi-Yagi antenna with a modified bow-tie driver for multi-band 3G/4G applications," *Progress In Electromagnetics Research C*, Vol. 71, 59–67, 2017.
24. Xu, K. D., D. T. Li, Y. H. Liu, and Q. H. Liu, "Printed quasi-yagi antennas using double dipoles and stub-loaded technique for multi-band and broadband applications," *IEEE Access*, Vol. 6, 31695–31702, Mar. 2018.
25. Aguilà, P., S. Zuffanelli, G. Zamora, F. Paredes, F. Martín, and J. Bonache, "Planar yagi-uda antenna array based on split-ring resonators (SRRs)," *IEEE Antennas Wireless Propag. Lett.*, Vol. 16, 1233–1236, May 2017.
26. Cai, X., W. Geyi, and H. C. Sun, "A printed dipole array with high gain and endfire radiation," *IEEE Antennas Wireless Propag. Lett.*, Vol. 16, 1512–1515, Jun. 2017.
27. Wen, G., *Foundations of Applied Electrodynamics*, 273–275, Wiley, New York, NY, USA, 2010.
28. Wen, G., *Foundations for Radio Frequency Engineering*, 410–420, World Scientific, 2015.
29. Jiang, Y. H., W. Geyi, L. S. Yang, and H. C. Sun, "Circularly-polarized focused microstrip antenna arrays," *IEEE Antennas Wireless Propag. Lett.*, Vol. 15, 52–55, Feb. 2016.
30. Sun, H. C. and W. Geyi, "Optimum design of wireless power transmission systems in unknown electromagnetic environments," *IEEE Access*, Vol. 5, 20198–20206, Oct. 2017.
31. Wan, W., W. Geyi, and S. Gao, "Optimum design of low-cost dual-mode beam-steerable arrays for customer-premises equipment applications," *IEEE Access*, Vol. 6, 16092–16098, Mar. 2018.
32. Cai, X. and W. Geyi, "An optimization method for the synthesis of flat-top radiation patterns in the near- and far-field regions," *IEEE Trans. Antennas Propag.*, Vol. 67, No. 2, 980–987, Feb. 2019.
33. Zuffanelli, S., G. Zamora, P. Aguilà, F. Paredes, F. Martín, and J. Bonache, "On the radiation properties of split-ring resonators (SRRs) at the second resonance," *IEEE Trans. Microw. Theory Techn.*, Vol. 63, No. 7, 2133–2141, Jul. 2015.